

BASIC RESEARCH PAPER

## ATG3-dependent autophagy mediates mitochondrial homeostasis in pluripotency acquirement and maintenance

Kun Liu<sup>a,b,†</sup>, Qian Zhao<sup>a,†</sup>, Pinglei Liu<sup>a,b,†</sup>, Jiani Cao<sup>a</sup>, Jiaqi Gong<sup>a,b</sup>, Chaoqun Wang<sup>a,c</sup>, Weixu Wang<sup>a,b</sup>, Xiaoyan Li<sup>a</sup>, Hongyan Sun<sup>a,b</sup>, Chao Zhang<sup>a,b</sup>, Yufei Li<sup>a,b</sup>, Minggui Jiang<sup>a,b</sup>, Shaohua Zhu<sup>a,b,d</sup>, Qingyuan Sun<sup>a</sup>, Jianwei Jiao<sup>a</sup>, Baoyang Hu<sup>a</sup>, Xiaoyang Zhao<sup>a</sup>, Wei Li<sup>a</sup>, Quan Chen<sup>a</sup>, Qi Zhou<sup>a</sup>, and Tongbiao Zhao<sup>a</sup>

<sup>a</sup>State Key Laboratory of Stem Cell and Reproductive Biology, Institute of Zoology, Chinese Academy of Sciences, Beijing, China; <sup>b</sup>Graduate University of Chinese Academy of Sciences, Beijing, China; <sup>c</sup>School of Biological Sciences, Qufu Normal University, Qufu, China; <sup>d</sup>School of Biological Sciences, University of Science and Technology of China, Hefei, China

### ABSTRACT

Pluripotent stem cells, including induced pluripotent and embryonic stem cells (ESCs), have less developed mitochondria than somatic cells and, therefore, rely more heavily on glycolysis for energy production.<sup>1–3</sup> However, how mitochondrial homeostasis matches the demands of nuclear reprogramming and regulates pluripotency in ESCs is largely unknown. Here, we identified ATG3-dependent autophagy as an executor for both mitochondrial remodeling during somatic cell reprogramming and mitochondrial homeostasis regulation in ESCs. Dysfunctional autophagy by *Atg3* deletion inhibited mitochondrial removal during pluripotency induction, resulting in decreased reprogramming efficiency and accumulation of abnormal mitochondria in established iPSCs. In *Atg3* null mouse ESCs, accumulation of aberrant mitochondria was accompanied by enhanced ROS generation, defective ATP production and attenuated pluripotency gene expression, leading to abnormal self-renewal and differentiation. These defects were rescued by reacquisition of wild-type but not lipidation-deficient *Atg3* expression. Taken together, our findings highlight a critical role of ATG3-dependent autophagy for mitochondrial homeostasis regulation in both pluripotency acquirement and maintenance.

### ARTICLE HISTORY

Received 19 January 2016  
Revised 21 June 2016  
Accepted 11 July 2016

### KEYWORDS

ATG3; mitochondria; mitophagy; pluripotent stem cell; reprogramming

### Introduction

Pluripotent stem cells (PSCs), including induced pluripotent and embryonic stem cells (ESCs), hold great promise for regenerative medicine due to their unlimited self-renewal capability and their ability to differentiate into any cell types of 3 germ layers in our bodies. PSCs are characterized by their ability to self-renew, pluripotency, immortalization in culture, high proliferation rate, and short G<sub>1</sub> phase.<sup>4,5</sup> The maintenance of intracellular homeostasis in ESCs requires timely clearance of damaged organelles and toxic proteins, as well as quick synthesis of total biomass associated with their high proliferation rate. Autophagy is a conserved degradation pathway by which organelles and cytoplasm are sequestered and subsequently delivered to lysosomes for hydrolytic digestion.<sup>6,7</sup> Autophagy serves as a protective strategy to eliminate toxic cytoplasmic contents, preventing cellular damage in response to stress.<sup>8</sup> In addition, autophagy also serves as a dynamic recycling system that produces new building blocks and bioenergy to fuel cellular renovation and homeostasis during normal development and differentiation.<sup>6,9</sup>

Mitochondria are dynamic double-membrane organelles that play critical roles in multiple biological processes, such





as energy production, apoptosis, and signal transduction.<sup>10,11</sup>

To meet the different bioenergetic demands of distinct cell types, cells regulate mitochondrial homeostasis through either biogenesis and degradation or dynamic fusion and fission.<sup>12</sup> Nuclear reprogramming induces both structural and functional remodeling of parental mitochondria in somatic cells to a state typical of ESCs.<sup>13,14</sup> However, how mitochondrial remodeling matches the requirements of somatic reprogramming and how ESCs harness their mitochondria to regulate pluripotency and self-renewal have not been clearly defined. Herein, we have determined that ATG3-dependent autophagy is an executor for both mitochondrial remodeling during reprogramming and mitochondrial homeostasis regulation in ESCs, and is pivotal for pluripotency acquirement and maintenance.

### Results


#### Mitochondria are removed during reprogramming

During the acquisition of pluripotency, specific mitochondrial remodeling must occur to meet the energetic and anabolic

**CONTACT** Qi Zhou  [qzhou@ioz.ac.cn](mailto:qzhou@ioz.ac.cn)  Institute of Zoology Chinese Academy of Sciences #D115, 1 Beichen West Road, Chaoyang District, Beijing 100101, P.R. China; Tongbiao Zhao  [tbzhao@ioz.ac.cn](mailto:tbzhao@ioz.ac.cn)  Institute of Zoology Chinese Academy of Sciences #E108, 1 Beichen West Road, Chaoyang District, Beijing 100101, P.R. China.

Color versions of one or more of the figures in the article can be found online at [www.tandfonline.com/kaup](http://www.tandfonline.com/kaup).

<sup>†</sup>These authors contributed equally to this work.

 Supplemental data for this article can be accessed on the publisher's website.

requirements of the pluripotent states. To examine how mitochondria are remodeled during reprogramming, we first monitored changes in mitochondrial morphology and number using transmission electron microscopy and mitochondrial mass using MitoTracker staining of mouse embryonic fibroblasts (MEFs) and PSCs. While mitochondria in MEFs possess well-developed morphology with dense cristae and an elongated shape, PSC mitochondria have an immature morphology with a globular shape and low-density cristae (Fig. 1A). Furthermore, the number of mitochondria in PSCs was significantly lower than that in MEFs (Fig. 1B). Accordingly, the total mitochondrial mass in PSCs was significantly lower than that of MEFs (Fig. 1C). Then, we isolated FUT4/SSEA-1-positive cells at reprogramming d 10 and iPSCs for mitochondrial mass and mtDNA copy number determination (Fig. 1D). The established iPSCs have normal karyotype, express pluripotent markers, form teratomas and contribute to chimeric mice, supporting their pluripotency (Fig. S1). The total mitochondrial mass of reprogramming cells gradually decreased in parallel with reprogramming progression (Fig. 1E), indicating mitochondria are removed during reprogramming. In support of these

observations, a quantitative polymerase chain reaction (PCR) assay using mitochondrial DNA (mtDNA) as a template was performed to track mtDNA copy number changes during reprogramming. As expected, genomic mtDNA gradually decreased as reprogramming progressed, confirming removal of mitochondria during this process (Fig. 1F).

### Autophagy is an executor of mitochondria removal during reprogramming

Because autophagy degrades both proteins and organelles, we next assessed whether autophagy was involved in mitochondrial removal during reprogramming. The autophagy inhibitors 3-methyladenine (3-MA) and bafilomycin A<sub>1</sub> (Baf-A1) were added at the beginning of reprogramming for 3 d to block autophagic flux. Interestingly, both 3-MA and Baf-A1 treatments significantly inhibited mitochondrial removal without affecting proliferation and apoptosis, indicating autophagy contributes to mitochondrial removal during reprogramming (Fig. 1G;

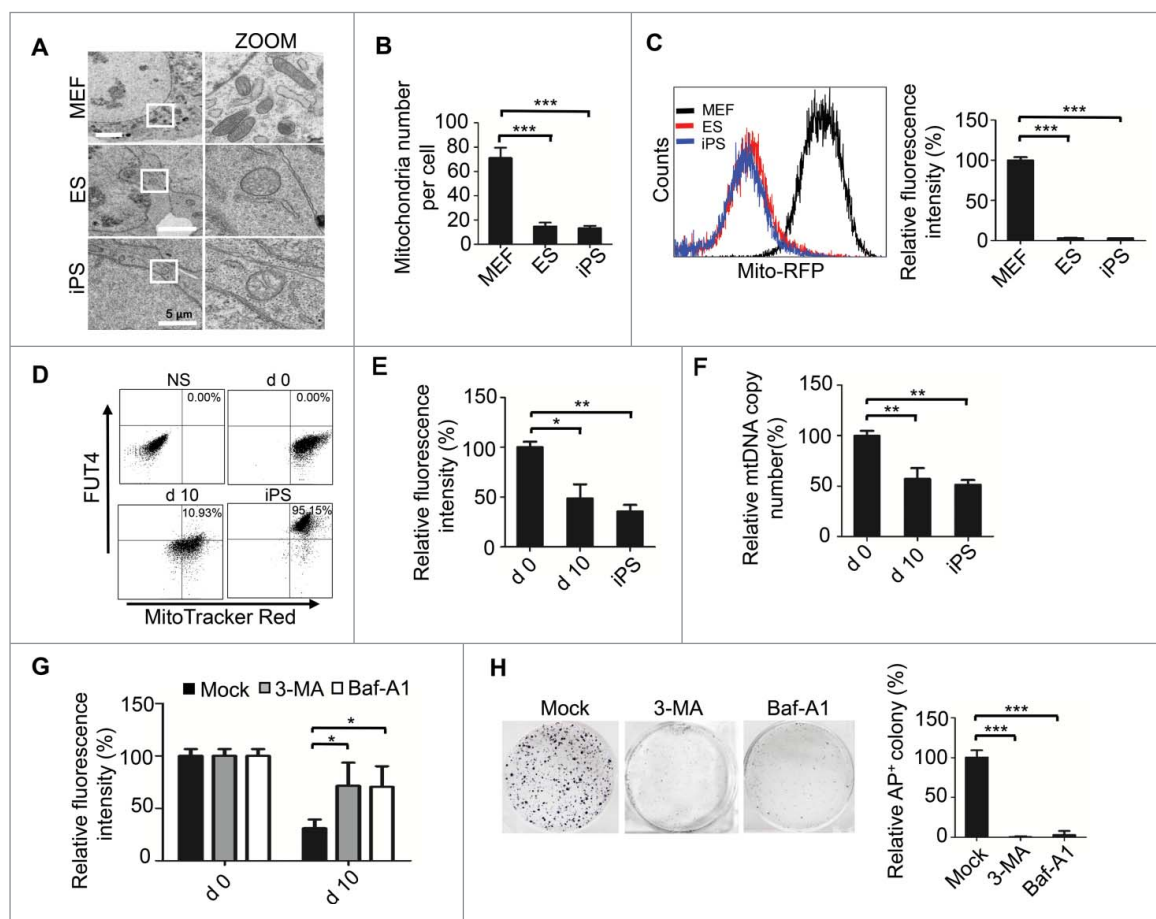


**Figure 1.** Mitochondrial numbers gradually decrease during reprogramming. (A) Representative transmission electronic microscopy images of mitochondria in MEFs, ESCs, and iPSCs. Bar: 5  $\mu$ m. (B) MEFs had more mitochondria than ESCs and iPSCs. Mean  $\pm$  error of mitochondria in (A) from 3 independent experiments,  $n = 3$ ; \*\*\*,  $P < 0.001$ ; Student  $t$  test. (C) MEFs had more total mitochondrial mass than ESCs or iPSCs. MEFs, ESCs and iPSCs derived from B6D2-Tg (CAG/Su9-DsRed2, Acr3-EGFP) mice were used for mitochondrial mass (Mito-mass) determination. Data expressed as mean  $\pm$  standard deviation (SD),  $n = 3$ ; \*\*\*,  $P < 0.001$ ; Student  $t$  test. (D) FUT4-positive cells were selected and used for mitochondrial mass or mtDNA copy number determination in (E, F) and G. Reprogramming cells at the indicated time points and iPSC were stained with FUT4 and MitoTracker Red, and analyzed by flow cytometry. (E) Mitochondrial mass gradually decreased during reprogramming. Data shown as mean  $\pm$  SD,  $n = 3$ ; \*,  $P < 0.05$ ; \*\*,  $P < 0.01$ ; Student's  $t$  test. (F) mtDNA copy numbers decreased during reprogramming. Data shown as mean  $\pm$  SD,  $n = 3$ ; \*\*,  $P < 0.01$ ; Student  $t$  test. (G) Inhibition of autophagy by 3-MA or Baf-A1 restricted mitochondrial decrease during reprogramming. Data expressed as mean  $\pm$  SD,  $n = 3$ ; \*,  $P < 0.05$ ; Student  $t$  test. (H) Alkaline phosphatase (AP) staining of iPSC colonies with 3-MA (5 mM) or Baf-A1 (5 nM) treatment during reprogramming. Data shown as mean  $\pm$  SD,  $n = 3$ ; \*\*\*,  $P < 0.001$ ; Student  $t$  test.

Fig. S2A and S2B). As a result, reprogramming efficiency was significantly reduced by 3-MA and Baf-A1 treatments (Fig. 1H).

ATG3 is a membrane-curvature sensor and plays a key role in autophagosome formation.<sup>15,16</sup> To further investigate whether autophagy directly contributes to mitochondrial remodeling during reprogramming, we isolated both *Atg3*<sup>+/+</sup> and *atg3*<sup>-/-</sup> MEFs (Fig. 2A). *Atg3* deletion did not affect MEF proliferation and apoptosis (Fig. S2C and S2D). Unlike wild-type *Atg3*<sup>+/+</sup> MEFs, we did not observe autophagosomes containing mitochondria in *atg3*<sup>-/-</sup> knockouts upon treatment with carbonyl cyanide-4-(trifluoromethoxy)phenylhydrazone (FCCP), indicating a lack of autophagy-mediated mitochondrial removal in *atg3*<sup>-/-</sup> MEFs (Fig. S3A). We then transfected *Atg3*<sup>+/+</sup> and *atg3*<sup>-/-</sup> MEFs with Yamanaka factors and monitored mitochondrial removal during reprogramming. Upon reprogramming initiation, mitophagy activation in *Atg3*<sup>+/+</sup> but not *atg3*<sup>-/-</sup> MEFs was observed (Fig. 2B, C; Fig. S3B). Although a decrease in the number of mitochondria occurred during reprogramming in both

*Atg3*<sup>+/+</sup> and *atg3*<sup>-/-</sup> MEFs, the relative decrease of mitochondria in wild-type MEFs was significantly higher than that of *atg3*<sup>-/-</sup> MEFs, indicating ATG3-dependent mitophagy contributes to mitochondrial remodeling during reprogramming (Fig. 2D; Fig. S3C). Accordingly, the reprogramming efficiency was significantly inhibited (Fig. 2G).

### ATG3-dependent autophagy is required for mitochondrial remodeling and successful reprogramming

An amphipathic helix domain at the N-terminus of ATG3 is responsible for membrane-curvature sensing and is critical for lipidation of the MAP1LC3/GABARAP family of autophagy proteins.<sup>15</sup> Mutation of this domain leads to failure of autophagosome formation.<sup>15</sup> To further confirm that impaired reprogramming of *atg3*<sup>-/-</sup> MEFs results from a defect in autophagy, gain-of-function assays were performed by overexpression of both wild-type and

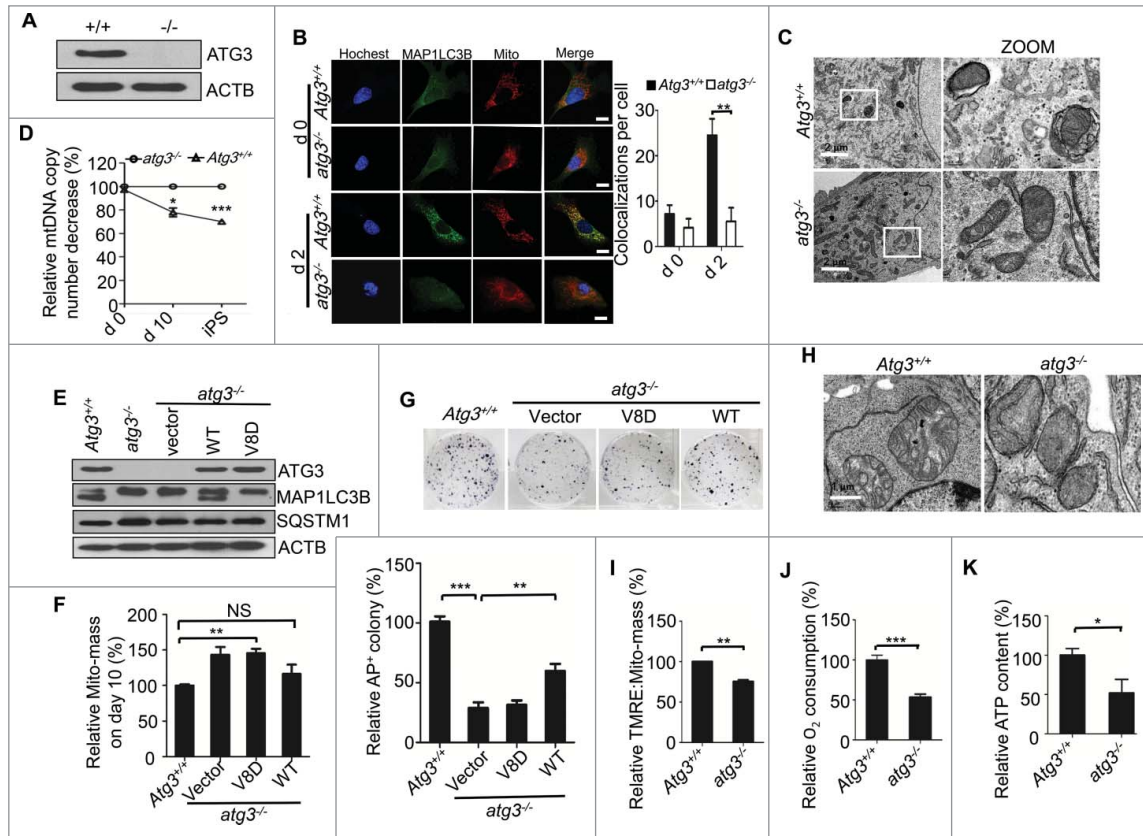


**Figure 2.** Lack of ATG3-dependent mitochondrial autophagy leads to defective reprogramming. (A) Western blot analysis of whole cell extracts from *Atg3*<sup>+/+</sup> and *atg3*<sup>-/-</sup> MEFs; ACTB served as a loading control. (B) Mitophagy in *Atg3*<sup>+/+</sup> and *atg3*<sup>-/-</sup> MEFs during iPSC induction. Blue: Hoechst 33342; Red: MitoTracker Red; Green: GFP-MAP1LC3B. Colocalizations of MAP1LC3B and mitochondria were counted in 50 cells. Data shown as mean  $\pm$  standard deviation (SD),  $n = 3$ ; \*\*,  $P < 0.01$ ; Student  $t$  test. (C) Representative transmission electronic microscopy images of autophagic mitochondria in reprogramming *Atg3*<sup>+/+</sup> and *atg3*<sup>-/-</sup> MEFs. Bar: 2  $\mu$ m. (D) Mitochondrial decreases were impaired by *Atg3* deletion during reprogramming. Data normalized to *atg3*<sup>-/-</sup> cells and shown as mean  $\pm$  standard deviation (SD),  $n = 3$ ; \*,  $P < 0.05$ ; \*\*\*,  $P < 0.001$ ; Student  $t$  test. (E) Defective autophagy in *atg3*<sup>-/-</sup> MEFs was rescued by reacquisition of wild-type *Atg3* expression. The indicated cells were starved for 2 h and then harvested for western blot using anti-ATG3, anti-MAP1LC3B, anti-SQSTM1 and anti-ACTB antibodies. (F) Elevated Mito-mass in *atg3*<sup>-/-</sup> reprogramming MEFs was recovered by wild-type *Atg3* expression. Data normalized to *Atg3*<sup>+/+</sup> cells and shown as mean  $\pm$  SD,  $n = 3$ ; \*\*,  $P < 0.01$ ; Student  $t$  test; NS, not significant. (G) Reacquisition of wild-type but not V8D mutant *Atg3* expression in *atg3*<sup>-/-</sup> cells compensated for reprogramming efficiency. Data shown as mean  $\pm$  SD,  $n = 3$ ; \*\*,  $P < 0.01$ ; \*\*\*,  $P < 0.001$ ; Student  $t$  test. (H) Representative transmission electronic microscopy images of mitochondria in *Atg3*<sup>+/+</sup> and *atg3*<sup>-/-</sup> iPSCs, Bar: 1  $\mu$ m. (I) Mitochondrial membrane potential was significantly reduced in *atg3*<sup>-/-</sup> iPSCs in contrast to *Atg3*<sup>+/+</sup> iPSCs. Data normalized to *Atg3*<sup>+/+</sup> cells and shown as mean  $\pm$  standard deviation (SD),  $n = 3$ ; \*\*,  $P < 0.01$ ; Student  $t$  test. (J) *atg3*<sup>-/-</sup> iPSCs have a significantly lower oxygen consumption rate than *Atg3*<sup>+/+</sup> iPSCs. Data normalized to *Atg3*<sup>+/+</sup> cells and shown as mean  $\pm$  SD,  $n = 3$ ; \*\*,  $P < 0.01$ ; Student  $t$  test. (K) *atg3*<sup>-/-</sup> iPSCs have a significant lower ATP level than *Atg3*<sup>+/+</sup> iPSCs. Data normalized to *Atg3*<sup>+/+</sup> cells and shown as mean  $\pm$  SD,  $n = 3$ ; \*,  $P < 0.05$ ; Student's  $t$  test.

lipidation-deficient *Atg3<sup>V8D</sup>* in *atg3<sup>-/-</sup>* MEFs (Fig. 2E). We found ectopic expression of wild-type *Atg3* but not lipidation-deficient mutant *Atg3<sup>V8D</sup>* in *atg3<sup>-/-</sup>* MEFs can rescue both defective mitochondrial clearance and reprogramming efficiency, supporting the view that ATG3-dependent autophagy is essential for mitochondrial remodeling and reprogramming (Fig. 2F, G).

We next investigated whether lack of ATG3-dependent autophagy affected the established iPSCs. By transmission electronic microscopy, we found that the abnormal mitochondria were accumulated in *Atg3*-deficient iPSCs and the mitochondrial cristae showed a blurred morphology (i.e., lack of clear definition) compared to *Atg3<sup>+/+</sup>* iPSCs (Fig. 2D, H). Further investigation identified significantly lower mitochondrial membrane potential and oxygen consumption, and compromised ATP production in *atg3<sup>-/-</sup>* versus *Atg3<sup>+/+</sup>* iPSCs, indicating the unsuccessful metabolic reprogramming of *atg3<sup>-/-</sup>* knock-outs (Fig. 2I, J, K). Taken together, these data support the conclusion that ATG3-dependent autophagy contributes to both reprogramming efficiency and reprogramming quality and is required for successful reprogramming.

### ATG3-dependent autophagy maintains ESC mitochondrial homeostasis and self-renewal

To investigate whether autophagy is involved in the regulation of mitochondrial dynamics and/or affects ESC identity, we first designed specific small interfering RNA (siRNA) targeting the autophagy regulator *Atg3* and found transient inhibition of this gene leads to ESC differentiation and loss of pluripotent gene expression (Fig. S4A-C). Then, we treated ESCs with 3-MA and found autophagy inhibition significantly affected ESC self-renewal (Fig. S4D). These data suggest the involvement of autophagy in ESC identity maintenance. To further investigate how autophagy regulates mitochondrial dynamics in ESC and thereby affects ESC identity, *Atg3<sup>+/+</sup>* and *atg3<sup>-/-</sup>* ESCs were isolated from the blastocyst of mice at embryonic d 3.5 (Fig. 3A). Upon FCCP treatment, we detected mitochondria associated with autophagic structures in wild-type *Atg3<sup>+/+</sup>* but not *atg3<sup>-/-</sup>* ESCs (Fig. 3B; Fig. S5B and S5C), indicating a lack of ATG3-dependent mitophagy in *atg3<sup>-/-</sup>* ESCs. Meanwhile, abnormal accumulation of mitochondria was detected in *atg3<sup>-/-</sup>* ESCs, as indicated by the existence of increased

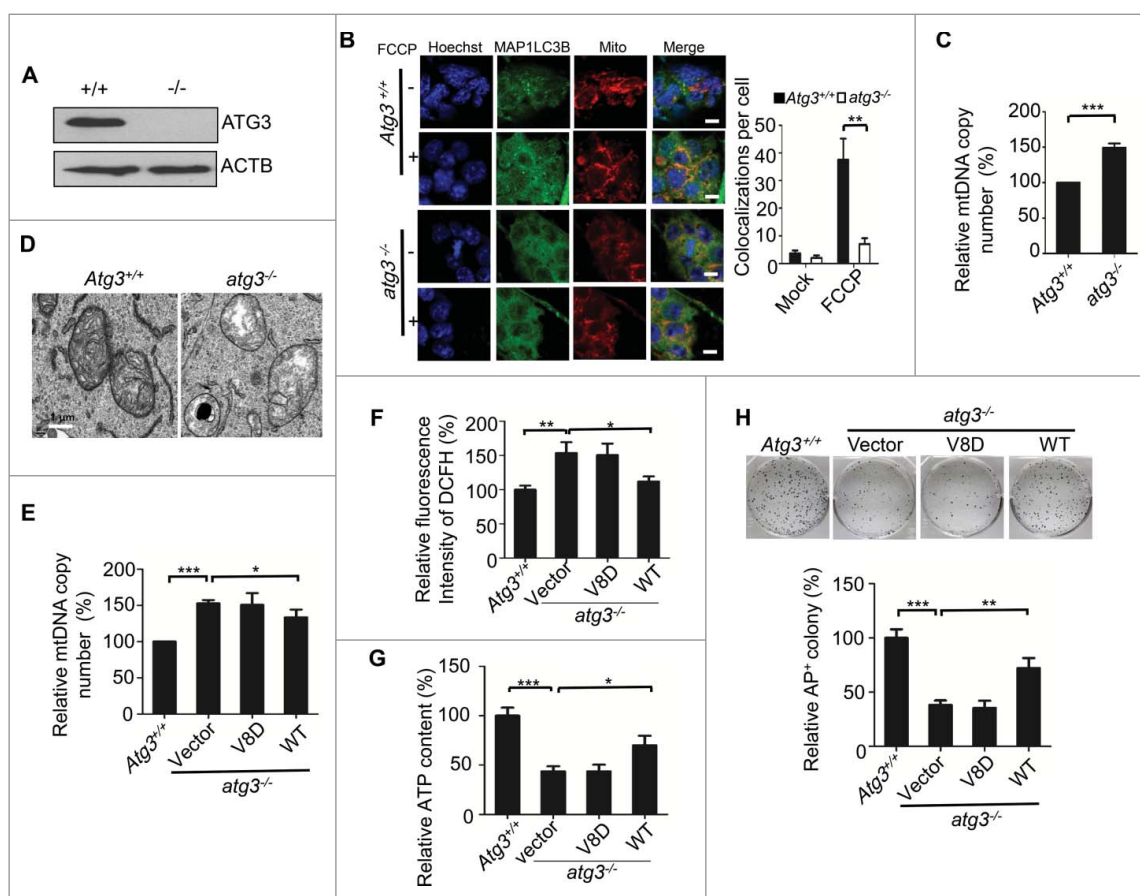


**Figure 3.** ATG3 regulates ESC mitochondrial homeostasis and self-renewal. (A) Western blot analysis of whole cell extracts from *Atg3<sup>+/+</sup>* and *atg3<sup>-/-</sup>* ESCs; ACTB served as a loading control. (B) Lack of FCCP-induced mitophagy in *atg3<sup>-/-</sup>* ESCs. Green: MAP1LC3B; Red: MitoTracker Red; Blue: Hoechst 33342. Colocalizations of LC3 and mitochondria were counted in 50 cells. Data shown as mean  $\pm$  SD,  $n = 3$ ; \*\*,  $P < 0.01$ ; Student *t* test. (C) Mitochondria accumulated in *atg3<sup>-/-</sup>* ESCs. Data presented as the mean of 3 independent experiments normalized to *Atg3<sup>+/+</sup>* ESCs and shown as mean  $\pm$  standard deviation (SD),  $n = 3$ ; \*\*\*,  $P < 0.001$ ; Student *t* test. (D) Transmission electronic microscopy images of mitochondria in *Atg3<sup>+/+</sup>* and *atg3<sup>-/-</sup>* ESCs. (E) Increased mtDNA copy number in *atg3<sup>-/-</sup>* ESCs was rescued by gain of wild-type but not V8D mutant *Atg3* expression. Data were normalized to *Atg3<sup>+/+</sup>* ESCs and shown as mean  $\pm$  SD,  $n = 3$ ; \*,  $P < 0.05$ ; \*\*,  $P < 0.01$ ; \*\*\*,  $P < 0.001$ ; Student *t* test. (F) The enhanced ROS generation in *atg3<sup>-/-</sup>* ESCs was rescued by reacquisition expression of WT but not V8D mutant *Atg3*. Data normalized to *Atg3<sup>+/+</sup>* ESCs and shown as mean  $\pm$  SD,  $n = 3$ ; \*,  $P < 0.05$ ; \*\*,  $P < 0.01$ ; Student *t* test. (G) Defective ATP generation in *atg3<sup>-/-</sup>* ESCs was partially rescued by gain of wild-type but not V8D mutant *Atg3*. Data normalized to *Atg3<sup>+/+</sup>* ESCs and shown as mean  $\pm$  SD,  $n = 3$ ; \*,  $P < 0.05$ ; \*\*\*,  $P < 0.001$ ; Student *t* test. (H) Aberrant self-renewal of *atg3<sup>-/-</sup>* ESCs was partially rescued by reacquisition of wild-type but not V8D mutant *Atg3* expression. Data shown as mean  $\pm$  SD,  $n = 3$ ; \*\*,  $P < 0.01$ ; \*\*\*,  $P < 0.001$ ; Student's *t* test.

mtDNA copy number, blurred-cristae mitochondria accumulation, enhanced ROS production and decreased ATP generation in *atg3<sup>-/-</sup>* ESCs (Fig. 3C–G). These data suggest ATG3-dependent autophagy plays critical roles to maintain mitochondrial homeostasis in ESCs. As a result, the clonogenic survival of *atg3<sup>-/-</sup>* ESCs was significantly impaired, indicating ATG3-dependent autophagic mitochondria removal is pivotal to ESC self-renewal (Fig. 3H).

To further confirm whether the abnormal accumulation of mitochondria and aberrant self-renewal ability of *atg3<sup>-/-</sup>* ESCs was directly caused by the loss of ATG3-mediated mitophagy, gain-of-function assays were performed by introducing *Atg3* expression into *atg3<sup>-/-</sup>* ESCs. We established stable *atg3<sup>-/-</sup>* ESC lines carrying an empty vector, wild-type *Atg3*, and mutant *Atg3<sup>V8D</sup>*. As expected, MAP1LC3B-II was only detected in *atg3<sup>-/-</sup>* stable ESC lines carrying wild-type *Atg3* but not the empty vector or *Atg3<sup>V8D</sup>* mutant upon starvation, demonstrating recovery of autophagy in *atg3<sup>-/-</sup>* ESCs by expression of wild-type *Atg3* (Fig. S5A). Meanwhile, mitophagosomes were again detected in *atg3<sup>-/-</sup>* ESCs expressing wild-type *Atg3* upon FCCP treatment (Fig. S5B). Consequently, the increased mtDNA copy number in *atg3<sup>-/-</sup>* ESCs was significantly

reduced by gain of wild-type *Atg3* expression, indicating accumulation of mitochondria in *Atg3*-deficient ESCs was directly caused by defects in ATG3-dependent mitochondrial autophagy (Fig. 3E). Furthermore, ROS production and ATP generation were also rescued by reacquisition expression of wild-type but not V8D mutant *Atg3* (Fig. 3F, G). Accordingly, the abnormal self-renewal of *Atg3*-deficient ESCs was compensated by reintroducing wild-type *Atg3* but not lipidation-deficient *Atg3<sup>V8D</sup>* mutant (Fig. 3H). Together, these data suggest that ATG3-dependent canonical autophagy maintains ESC mitochondrial homeostasis and self-renewal.

### ATG3-dependent autophagy regulates ESC pluripotency and differentiation

Differentiation of PSCs requires a specific remodeling process involving an increase in mitochondrial numbers. To test whether autophagy is involved in this process, we performed an embryonic body (EB) differentiation assay. The number of mitochondria gradually increased during EB differentiation as expected (Fig. 4A). We next assessed EB differentiation using *Atg3<sup>+/+</sup>* and *atg3<sup>-/-</sup>* ESCs.

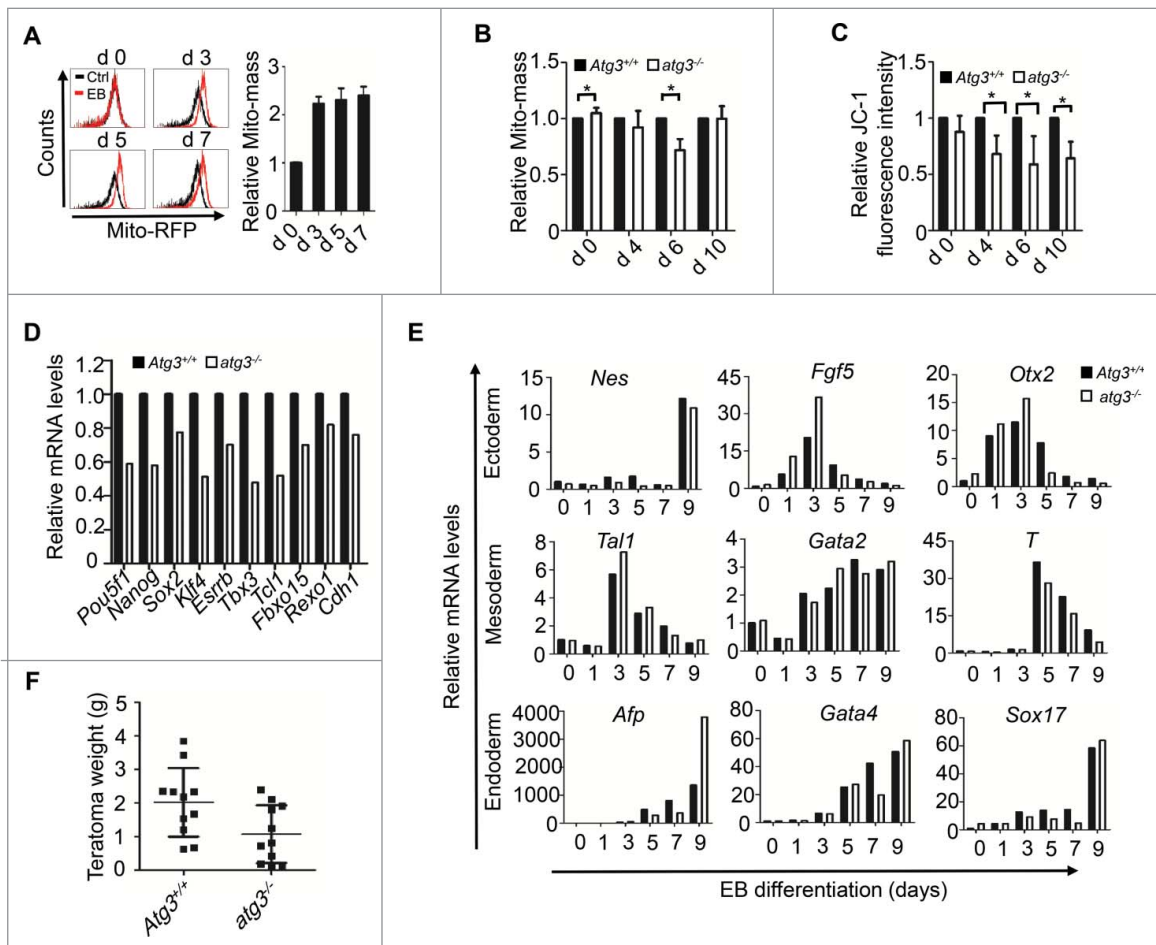


**Figure 4.** Loss of ATG3-mediated mitochondrial autophagy compromises ESC pluripotency and differentiation. (A) Mitochondrial mass (Mito-mass) increased during EB differentiation. Data presented as the mean  $\pm$  error from 3 independent experiments. (B) Mitochondrial mass increases during EB differentiation were impaired by *Atg3* deletion. Mean values were normalized to *Atg3<sup>+/+</sup>* EB,  $n = 3$ ; \*,  $P < 0.05$ ; Student *t* test. (C) *Atg3<sup>+/+</sup>* and *atg3<sup>-/-</sup>* ESC-formed EBs were analyzed by JC-1 staining at the indicated differentiation times. Mean values were normalized to *Atg3<sup>+/+</sup>* EB,  $n = 3$ ; \*,  $P < 0.05$ ; Student *t* test. (D) Transcription of pluripotency genes in ESCs was impaired by *Atg3* deletion. Data are representative of 3 independent experiments. (E) Lack of ATG3-dependent mitophagy impaired ESC lineage specification. Data shown are representative of 3 independent experiments. (F) *Atg3* deletion compromised ESC teratoma differentiation. Data from 3 independent experiment and shown as mean  $\pm$  SD.

Surprisingly, contrary to the relatively larger number of mitochondria in *atg3*<sup>-/-</sup> ESCs, the mitochondrial increase was delayed in *atg3*<sup>-/-</sup> ESCs compared to the wild-type during EB differentiation, indicating *atg3*<sup>-/-</sup> ESC mitochondria are abnormal and ATG3-dependent autophagy is crucial for mitochondrial remodeling during EB differentiation (Fig. 4B, C; Fig. S6A and S6B). Furthermore, decreased pluripotent gene expression was detected in *atg3*<sup>-/-</sup> vs. wild-type ESCs, suggesting elimination of ATG3-dependent autophagy leads to the compromised pluripotency in ESCs (Fig. 4D). In support of this assumption, *atg3*<sup>-/-</sup> ESCs showed abnormal EB differentiation, characterized by delayed expression of certain endodermic and mesodermic marker genes (Fig. 4E). Furthermore, a teratoma formation assay was employed to investigate the autophagy contribution to ESC differentiation. While both *Atg3*<sup>+/+</sup> and *atg3*<sup>-/-</sup> ESCs formed teratomas, the average weight of teratomas formed by *Atg3*<sup>+/+</sup> ESCs is significantly larger than that of *atg3*<sup>-/-</sup> ESCs, supporting the view that ATG3-dependent autophagy is critical for differentiation of pluripotent stem cells (Fig. 4F). Together, these data suggest ATG3-dependent autophagy is involved in mitochondrial remodeling during ESC differentiation and regulates ESC pluripotency and differentiation.

## Discussion

In somatic cells, damaged or superfluous mitochondria are selectively recognized and sequestered by phagophores, followed by mitophagosomal fusion with lysosomes and autophagic degradation, a process called mitophagy.<sup>17-19</sup> However, how mitochondrial homeostasis is regulated in PSCs is largely unknown. By using an *Atg3* knockout model system, we demonstrate that ATG3-dependent autophagy is required for mitochondrial homeostasis regulation in both pluripotency acquisition and maintenance, and plays pivotal roles for ESC differentiation.

Somatic cell reprogramming remodels cellular components and organelles, as well as metabolism patterns. Transition of somatic cell oxidative phosphorylation to glycolysis through downregulation of mitochondrial respiratory chain complexes and upregulation of glycolytic genes has been identified as a critical event during reprogramming.<sup>20</sup> In agreement with this model, a PDK1/phosphoinositide-dependent kinase-1 activator, which facilitates the metabolic conversion from oxidative phosphorylation to glycolysis, in combination with POU5F1/OTF3 and a couple of small molecules could successfully induce pluripotency.<sup>21</sup> However, how mitochondria remodel themselves to facilitate the metabolic switching in somatic cell reprogramming is not clear.

Mitochondria number and structure in PSCs were dramatically changed compared to somatic fibroblasts, suggesting a total mitochondrial remodeling process must occur during reprogramming. Although mitochondrial removal has been proposed to be required for nuclear reprogramming, the detailed mechanisms driving this remodeling process have not been clearly defined. Mitochondrial fission and fusion have been proposed to be responsible for mitochondrial remodeling during reprogramming.<sup>22,23</sup> Inhibition of mitochondrial fission regulator DNMI1 (dynamins 1-like) expression significantly decreased reprogramming efficiency, indicating the potential involvement of mitophagy in somatic cell reprogramming.<sup>23</sup> Conversely, a recent study has demonstrated an ATG5-independent noncanonical mitophagy involvement in somatic

reprogramming through ULK1 (unc-51 like kinase 1) and RAB9 pathway.<sup>24</sup> In contrast, we have demonstrated that ATG3-dependent canonical autophagy contributes to mitochondrial remodeling and regulates reprogramming. Although *Atg3* deletion did not completely block mitochondrial clearance and iPSC colony formation, the abnormal mitochondria accumulated in established *atg3*<sup>-/-</sup> iPSCs compared to *Atg3*<sup>+/+</sup> iPSCs, leading to enhanced ROS generation and defective metabolic reprogramming. These data support the hypothesis that ATG3-dependent canonical autophagy regulates both mitochondrial quantity and quality and is critical for successful reprogramming. Consistent with this notion, recent studies have shown that transient activation of autophagy through MTOR (mechanistic target of rapamycin [serine/threonine kinase]) suppression either by SOX2 (SRY [sex determining region Y]-box 2) or rapamycin is a critical early step for successful reprogramming.<sup>25</sup>

Mitochondrial dynamics (fusion and fission) and mitophagy have been proposed to be important players for mitochondrial homeostasis regulation in somatic cells.<sup>12</sup> Recent studies have shown that the mitochondrial fusion protein GFER (growth factor, *erv1* [*S. cerevisiae*]-like (augmenter of liver regeneration)), which is highly expressed in ESCs, modulates the mitochondrial fission GTPase DNMI1 to preserve mouse ESC mitochondrial homeostasis and function, and maintain pluripotency in ESCs.<sup>26</sup> Knockdown of *Gfer* in ESCs leads to decreased pluripotent marker gene expression accompanied by excessive mitochondrial fragmentation and mitochondrial autophagy, indicating the involvement of mitochondrial dynamics in mitochondrial homeostasis and pluripotency regulation in mouse ESCs.<sup>26</sup> By using *atg3*<sup>-/-</sup> ESCs, we demonstrate here that ATG3-dependent autophagy is required for ESC mitochondrial homeostasis and ESC identity maintenance. ESCs are endowed with high rates of catabolic processes to rapidly generate multiple building blocks for cellular reconstruction to meet their high proliferation rates. Furthermore, to maintain their identity, rapidly dividing ESCs have to efficiently remove damaged mitochondria to avoid the oxidative damage to their genomes. *Atg3* null mouse ESCs accumulate aberrant mitochondria accompanied by enhanced mitochondrial mass, and generate increased levels of ROS and decreased levels of ATP, leading to compromised self-renewal and pluripotency ability. Thus we propose ESCs employ autophagy, by which dysfunctional mitochondria and the resulting excessive ROS can be rapidly removed, to protect their genome from oxidative damage and thus maintain their self-renewal and pluripotency.

In somatic cells, mitochondria can be eliminated either through selective mitochondrial autophagy or nonselective autophagy.<sup>17</sup> The selective autophagic elimination of mitochondria has been extensively reported to be regulated by *PARK2* and *PINK1* (PTEN induced putative kinase 1).<sup>17,27-34</sup> We did not observe defective mitochondrial clearance and impaired reprogramming efficiency when we used *park2*<sup>-/-</sup> MEFs for the reprogramming assay, indicating *PARK2*-mediated selective mitochondrial autophagy was not involved in mitochondrial remodeling during reprogramming, and other unidentified mitophagy pathways may play a role in this process.

Our findings significantly contribute to the current understanding of reprogramming and/or ESC identity

maintenance in terms of mitochondrial homeostasis regulation, and may provide new strategies for directed differentiation of ESCs by manipulating autophagy. Furthermore, our data highlight the contribution of mitochondria in ESC identity maintenance. In the future, it would be of great interest to investigate how genes that mediate mitochondrial homeostasis are regulated by core pluripotency transcription factors in PSCs upon differentiation or, conversely, during reprogramming.

## Materials and methods

### Animals, reagents, antibodies, and plasmids

B6D2-Tg (CAG/Su9-DsRed2, Acr3-EGFP) RBGS002Osb (RBRC03743),<sup>35</sup> MAP1LC3B-GFP (RBRC00806),<sup>36</sup> and *Atg3*<sup>+/-</sup> (RBRC02761)<sup>16</sup> mice were purchased from Riken BioResource Center. All protocols used for animal manipulation were approved by the Institutional Animal Care Committee. JC-1 (40705ES03), MitoTracker Green (40742ES50), and MitoTracker Red (40743ES50) were purchased from Yeasen. The anti-MAP1LC3B antibody (Medical and Biological Laboratories Co., PM036) was used at 1:200; Alexa Fluor<sup>®</sup> 488 donkey anti-rabbit IgG (H<sup>+</sup>L) (Invitrogen Thermo Fisher Scientific, A21206) was used at 1:500; anti-ACTB (1:5000) was obtained from Sigma Aldrich (A5441); anti-SQSTM1/p62 (1:2000) were purchased from Abcam (ab56416); anti-ATG3 (1:500) was purchased from Cell Signaling Technology (3415S); SSEA-1 were bought from Santa Cruz Biotechnology (SC-21702AF488); 3-MA, chloroquine, Hoechst 33342, Baf-A1, and anti-MAP1LC3B (1:2000) were obtained from Sigma Aldrich (M9281, C6628, B2261, B1793, L7543). pMXs-*Pou5f1*, pMXs-*Sox2*, pMXs-*Klf4*, and pMXs-*cMyc* were purchased from Addgene (13366, 13367, 13370, 13375; Deposited by Shinya Yamanaka lab). *Atg3* and its lipidation-deficient V8D mutant were cloned into pMXs and pCDH-CAG-RFP lenti-vectors as described previously.<sup>15</sup>

### ESC isolation and iPSC induction

*Atg3*<sup>+/+</sup> and *atg3*<sup>-/-</sup> ESCs were isolated at embryonic d 3.5 and cultured on feeder layers for 5 d using 2i medium (ESC medium with 1  $\mu$ M PD0325901 [Stemgent, 040006], 3  $\mu$ M CHIR99021 [Stemgent, 040004] and 1000 U/ml leukemia inhibitory factor [Merck Millipore, ESG1107]). Then, ESC colonies were selected and cultured for 3 to 5 passages. After, isolated ESCs were routinely maintained in ESC medium (knockout Dulbecco's modified Eagle's medium [Gibco Life Technologies, 10829018] with 15% fetal bovine serum [GE Healthcare Life Sciences, sh30070.03], 2 mM glutamine [Gibco Life Technologies, 25030164], 1 mM sodium pyruvate [Gibco Life Technologies, 11360070], 0.1 mM nonessential amino acids [Gibco Life Technologies, 11140050], 100  $\mu$ g/ml streptomycin and 100 U/ml penicillin [Gibco Life Technologies, 15140122], 0.055 mM  $\beta$ -mercaptoethanol [Gibco Life Technologies, 21985023], and 1000 U/ml leukemia inhibitory factor [Merck Millipore, ESG1107]). For iPSC generation, MEFs were seeded at 50,000 cells/well in a 6-well plate and infected with a retrovirus cocktail expressing *Pou5f1/Oct4*, *Sox2*, *Klf4*, and *Myc*; iPSC colonies were picked 14 d after infection as described previously.<sup>37</sup>

### The mtDNA copy number and mitochondrial mass detection

For mtDNA copy number determination, total DNA was extracted by a TIANamp Genomic DNA Kit (Tiangen Biotech [Beijing] Co., DP304-03). The mtDNA copy number was detected by quantitative real-time PCR using genomic DNA as a loading control. The primers used were published previously.<sup>38</sup> Primers for genomic DNA (H19) were 5'-GTCCACGAGACCAATGACTG-3' (reverse) and 5'-GTACCCACCTGTCGTC-3' (forward); mtDNA (CytB) primers were 5'-ATTCTTCATGTCGGACGAG-3' (reverse) and 5'-ACTGA-GAAGCCCCCTCAAAT-3' (forward). For total mitochondrial mass detection, cells were digested into single cell suspensions by trypsin (Gibco Life Technologies, 25200072), stained with 100 nM MitoTracker Green/Red for 30 min at 37°C, then washed and analyzed by a FACS calibur flow cytometer (BD Biosciences, Shanghai).

### Measurement of OCR, ROS and ATP

Measurement of intact cellular respiration was performed using a Seahorse XF24 analyzer (Seahorse Bioscience Asia, Shanghai). Briefly, ESC or MEF cells were seeded at 60,000 cells/well 6 h before measurements. Then respiration was measured and determined using a standard protocol in the manual. The cellular ATP content was determined using a CellTiter-GloLuminescent Cell Viability Assay kit (Promega Corporation, 0000092970). The cellular ROS was measured by flow cytometry using HDCF-DA from Sigma Aldrich (D6883).

### Immunofluorescence microscopy

The immunostaining was performed as previously described.<sup>39</sup> Briefly, MEFs or ESCs cultured on gelatin-coated glass slides were fixed with 4% paraformaldehyde for 20 min, washed with Dulbecco's PBS (Corning Inc., R21-031-CV), permeabilized by 0.2% Triton-X100 (Sigma Aldrich, X100) for 0.5 h, blocked with 2% bovine serum albumin (Sigma Aldrich, A1933) for 1 h, stained with appropriate primary antibodies overnight at 4°C, and then incubated with secondary antibodies for 2 h at room temperature. Cell nuclei were counterstained with Hoechst 33342.

### Quantitative real-time PCR

Total RNA was extracted from MEFs, ESCs, iPSCs, and EBs with an RNeasy Total RNA Isolation Kit (Qiagen, 74104). Total RNA (1  $\mu$ g) was reverse transcribed into cDNA using a SuperScript<sup>™</sup> III First-Strand Synthesis System (Invitrogen Thermo Fisher Scientific, 18080051). The primers used were as reported previously.<sup>40</sup> *Pou5f1*: 5'-AGAGGATCACCTTGGGGTACA-3' (forward), 5'-CGAAGCGACAGATGGTGGTC-3' (reverse); *Nano*: 5'-TCTTCTGGTCCCCACAGTTT-3' (forward), 5'-GCAAGAAATAGTTCTCGGGATGAA-3' (reverse); *Sox2*: 5'-GCGGAGTGGAATCTTTGTCC-3' (forward), 5'-CGGGAAGCGGTG-TACTTATCCTT-3' (reverse); *Klf4*: 5'-GTGCCCC GACTA ACCGTTG-3' (forward), 5'-GTCGTTGAACTCCTCGGTCT-3' (reverse); *Esrrb*: 5'-CAG GCAAGGATGACAGACG-3'

(forward), 5'-GAGACAGCACGAAGGACTGC-3' (reverse); *Tbx3*: 5'-TTGCAAAGGGTTTTGAGAC-3' (forward), 5'-TGGAGGACTCATCCGAAGTC-3' (reverse); *Tcl1*: 5'-AAATTCCAGGTGATCTTGCG-3' (forward), 5'-TGTCCTTGGGGTACAGTTGC-3' (reverse); *Fbxo15*: 5'-TCGTGGGACTGAGCACTA-3' (forward), 5'-TGACAGATGAGCCTCTAACAAC-3' (reverse); *Rexo1*: 5'-CCCTCGACAGACTGACCC-TAA-3' (forward), 5'-TCGGG GCTAATCTCACTTTTCAT-3' (reverse); *Cdh1*: 5'-CAGGTCTCCTCATGGCTTTGC-3' (forward), 5'-CTTCCGAAAAGAAGGCTGTCC-3' (reverse); *Nes*: 5'-CCCTGAAGTCGAGGAGCTG-3' (forward), 5'-CTGCTGCACCTCTAAGCGA-3' (reverse); *Fgf5*: 5'-CTGTATGGACCACAGGGAGTAAC-3' (forward), 5'-ATTAAGCTCCTGGTTCGCAAG-3' (reverse); *Otx2*: 5'-TATC TAAAGCAA CCGCCTTACG-3' (forward), 5'-AAGTCCATACCCGAAGTGGTC-3' (reverse); *Tall1*: 5'-CTGGCCTCCAGCTACATTTCT-3' (forward), 5'-GTCACGGTCTTTGCTCAACTT-3' (reverse); *Gata2*: 5'-CACCCCGCCGTATTGAATG-3' (forward), 5'-CCTGCGAGTCGAGATGGTTG-3' (reverse); *T*: 5'-GCTTCAA GGAGCTAACTAACGAG-3' (forward), 5'-CCAGCAAGAAAGAG TACATGGC-3' (reverse); *Afp*: 5'-CTTCCCTCATCCTCCTGCTAC-3' (forward), 5'-ACAAA CTGGGTAAAGGTGATGG-3' (reverse); *Gata4*: 5'-CCCTACCCAGCCTACATGG-3' (forward), 5'-ACATATCGAGATTGGGGTGTCT-3' (reverse); *Sox17*: 5'-GATGCGGGATACGCCAGTG-3' (forward), 5'-CCACCACCTCGCCTTTTCAC-3' (reverse); *Actb*: 5'-GGCTGTATTCCTC CATCG-3' (forward), 5'-CCAGTTG GTAACAATGCCATGT-3' (reverse).

## Abbreviations

3-MA	3-methyladenine
ATG3	autophagy-related 3
ATP	adenosine triphosphate
Baf-A1	bafilomycin A <sub>1</sub>
EB	embryonic body
ESC	embryonic stem cells
FCCP	carbonyl cyanide 4-(trifluoromethoxy) phenylhydrazide
iPSC	induced pluripotent stem cell
MEFs	mouse embryonic fibroblasts
mtDNA	mitochondrial DNA
PSC	pluripotent stem cell
ROS	reactive oxygen species

## Disclosure of potential conflicts of interest

No potential conflicts of interest were disclosed.

## Acknowledgments

We thank G.W., at our institute, T.Z., J.L. and L.C. at IM-CAS for technical supports.

## Funding

This work was supported by grants from the Strategic Priority Research Program of the Chinese Academy of Sciences XDA01040108, the China National Basic Research Program 2012CB966901, the National Natural

Science Foundation of China Program 31271592, 31570995, and National Thousand Young Talents Program to T.Z.

## References

- Zhang J, Nuebel E, Daley GQ, Koehler CM, Teitell MA. Metabolic regulation in pluripotent stem cells during reprogramming and self-renewal. *Cell Stem Cell* 2012; 11:589-95; PMID:23122286; <http://dx.doi.org/10.1016/j.stem.2012.10.005>
- Vessoni AT, Muotri AR, Okamoto OK. Autophagy in stem cell maintenance and differentiation. *Stem Cells Dev* 2012; 21:513-20; PMID:22066548; <http://dx.doi.org/10.1089/scd.2011.0526>
- Suhr ST, Chang EA, Tjong J, Alcasid N, Perkins GA, Goissis MD, Ellisman MH, Perez GI, Cibelli JB. Mitochondrial rejuvenation after induced pluripotency. *PLoS One* 2010; 5:e14095; PMID:21124794; <http://dx.doi.org/10.1371/journal.pone.0014095>
- Ruiz S, Panopoulos AD, Herreras A, Bissig KD, Lutz M, Berggren WT, Verma IM, Izpisua Belmonte JC. A high proliferation rate is required for cell reprogramming and maintenance of human embryonic stem cell identity. *Curr Biol* 2011; 21:45-52; PMID:21167714; <http://dx.doi.org/10.1016/j.cub.2010.11.049>
- White J, Dalton S. Cell cycle control of embryonic stem cells. *Stem Cell Rev* 2005; 1:131-8; PMID:17142847; <http://dx.doi.org/10.1385/SCR.1.2.131>
- Mizushima N, Levine B. Autophagy in mammalian development and differentiation. *Nat Cell Biol* 2010; 12:823-30; PMID:20811354; <http://dx.doi.org/10.1038/ncb0910-823>
- He C, Klionsky DJ. Regulation mechanisms and signaling pathways of autophagy. *Annu Rev Genet* 2009; 43:67-93; PMID:19653858; <http://dx.doi.org/10.1146/annurev-genet-102808-114910>
- Orrenius S, Kaminsky VO, Zhivotovsky B. Autophagy in toxicology: cause or consequence? *Annu Rev Pharmacol Toxicol* 2012; 53:275-97; PMID:23072380; <http://dx.doi.org/10.1146/annurev-pharmtox-011112-140210>
- Mizushima N, Komatsu M. Autophagy: renovation of cells and tissues. *Cell* 2011; 147:728-41; PMID:22078875; <http://dx.doi.org/10.1016/j.cell.2011.10.026>
- Levine B, Klionsky DJ. Development by self-digestion: molecular mechanisms and biological functions of autophagy. *Dev Cell* 2004; 6:463-77; PMID:15068787; [http://dx.doi.org/10.1016/S1534-5807\(04\)00099-1](http://dx.doi.org/10.1016/S1534-5807(04)00099-1)
- Attardi G, Schatz G. Biogenesis of mitochondria. *Annu Rev Cell Biol* 1988; 4:289-333; PMID:2461720; <http://dx.doi.org/10.1146/annurev.cb.04.110188.001445>
- Westermann B. Mitochondrial fusion and fission in cell life and death. *Nat Rev Mol Cell Biol* 2010; 11:872-84; PMID:21102612; <http://dx.doi.org/10.1038/nrm3013>
- Liu K, Song Y, Yu H, Zhao T. Understanding the roadmaps to induced pluripotency. *Cell Death Dis* 2014; 5:e1232; PMID:24832604; <http://dx.doi.org/10.1038/cddis.2014.205>
- De Los Angeles A, Ferrari F, Xi R, Fujiwara Y, Benvenisty N, Deng H, Hochedlinger K, Jaenisch R, Lee S, Leitch HG, et al. Hallmarks of pluripotency. *Nature* 2015; 525:469-78; PMID:26399828; <http://dx.doi.org/10.1038/nature15515>
- Nath S, Dancourt J, Shteyn V, Puente G, Fong WM, Nag S, Bewersdorf J, Yamamoto A, Antonny B, Melia TJ. Lipidation of the LC3/GABARAP family of autophagy proteins relies on a membrane-curvature-sensing domain in Atg3. *Nat Cell Biol* 2014; 16:415-24; PMID:24747438; <http://dx.doi.org/10.1038/ncb2940>
- Sou YS, Waguri S, Iwata J, Ueno T, Fujimura T, Hara T, Sawada N, Yamada A, Mizushima N, Uchiyama Y, et al. The Atg8 conjugation system is indispensable for proper development of autophagic isolation membranes in mice. *Mol Biol Cell* 2008; 19:4762-75; PMID:18768753; <http://dx.doi.org/10.1091/mbc.E08-03-0309>
- Youle RJ, Narendra DP. Mechanisms of mitophagy. *Nat Rev Mol Cell Biol* 2011; 12:9-14; PMID:21179058; <http://dx.doi.org/10.1038/nrm3028>
- Tolkovsky AM. Mitophagy. *Biochim Biophys Acta* 2009; 1793:1508-15; PMID:19289147; <http://dx.doi.org/10.1016/j.bbamcr.2009.03.002>
- Lemasters JJ. Selective mitochondrial autophagy, or mitophagy, as a targeted defense against oxidative stress, mitochondrial dysfunction,



- and aging. *Rejuvenation Res* 2005; 8:3-5; PMID:15798367; <http://dx.doi.org/10.1089/rej.2005.8.3>
- [20] Folmes CD, Nelson TJ, Martinez-Fernandez A, Arrell DK, Lindor JZ, Dzeja PP, Ikeda Y, Perez-Terzic C, Terzic A. Somatic oxidative bioenergetics transitions into pluripotency-dependent glycolysis to facilitate nuclear reprogramming. *Cell Metab* 2011; 14:264-71; PMID:21803296; <http://dx.doi.org/10.1016/j.cmet.2011.06.011>
- [21] Zhu S, Li W, Zhou H, Wei W, Ambasadhan R, Lin T, Kim J, Zhang K, Ding S. Reprogramming of human primary somatic cells by OCT4 and chemical compounds. *Cell Stem Cell* 2010; 7:651-5; PMID:21112560; <http://dx.doi.org/10.1016/j.stem.2010.11.015>
- [22] Prigione A, Fauler B, Lurz R, Lehrach H, Adjaye J. The senescence-related mitochondrial/oxidative stress pathway is repressed in human induced pluripotent stem cells. *Stem Cells* 2010; 28:721-33; PMID:20201066; <http://dx.doi.org/10.1002/stem.404>
- [23] Vazquez-Martin A, Cufi S, Corominas-Faja B, Oliveras-Ferreros C, Vellon L, Menendez JA. Mitochondrial fusion by pharmacological manipulation impedes somatic cell reprogramming to pluripotency: new insight into the role of mitophagy in cell stemness. *Aging (Albany NY)* 2012; 4:393-401; PMID:22713507
- [24] Ma T, Li J, Xu Y, Yu C, Xu T, Wang H, Liu K, Cao N, Nie BM, Zhu SY, et al. Atg5-independent autophagy regulates mitochondrial clearance and is essential for iPSC reprogramming. *Nat Cell Biol* 2015; 17:1379-87; PMID:26502054; <http://dx.doi.org/10.1038/ncb3256>
- [25] Wang S, Xia P, Ye B, Huang G, Liu J, Fan Z. Transient activation of autophagy via Sox2-mediated suppression of mTOR is an important early step in reprogramming to pluripotency. *Cell Stem Cell* 2013; 13:617-25; PMID:24209762; <http://dx.doi.org/10.1016/j.stem.2013.10.005>
- [26] Todd LR, Damin MN, Gomathinayagam R, Horn SR, Means AR, Sankar U. Growth factor erv1-like modulates Drp1 to preserve mitochondrial dynamics and function in mouse embryonic stem cells. *Mol Biol Cell* 2010; 21:1225-36; PMID:20147447; <http://dx.doi.org/10.1091/mbc.E09-11-0937>
- [27] Deng H, Dodson MW, Huang H, Guo M. The Parkinson disease genes pink1 and parkin promote mitochondrial fission and/or inhibit fusion in *Drosophila*. *Proc Natl Acad Sci U S A* 2008; 105:14503-8; PMID:18799731; <http://dx.doi.org/10.1073/pnas.0803998105>
- [28] Poole AC, Thomas RE, Andrews LA, McBride HM, Whitworth AJ, Pallanck LJ. The PINK1/Parkin pathway regulates mitochondrial morphology. *Proc Natl Acad Sci U S A* 2008; 105:1638-43; PMID:18230723; <http://dx.doi.org/10.1073/pnas.0709336105>
- [29] Yang Y, Ouyang Y, Yang L, Beal MF, McQuibban A, Vogel H, Lu B. Pink1 regulates mitochondrial dynamics through interaction with the fission/fusion machinery. *Proc Natl Acad Sci U S A* 2008; 105:7070-5; PMID:18443288; <http://dx.doi.org/10.1073/pnas.0711845105>
- [30] Geisler S, Holmstrom KM, Skujat D, Fiesel FC, Rothfuss OC, Kahle PJ, Springer W. PINK1/Parkin-mediated mitophagy is dependent on VDAC1 and p62/SQSTM1. *Nat Cell Biol* 2010; 12:119-31; PMID:20098416; <http://dx.doi.org/10.1038/ncb2012>
- [31] Geisler S, Holmstrom KM, Treis A, Skujat D, Weber SS, Fiesel FC, Kahle PJ, Springer W. The PINK1/Parkin-mediated mitophagy is compromised by PD-associated mutations. *Autophagy* 2010; 6:871-8; PMID:20798600; <http://dx.doi.org/10.4161/auto.6.7.13286>
- [32] Springer W, Kahle PJ. Regulation of PINK1-Parkin-mediated mitophagy. *Autophagy* 2011; 7:266-78; PMID:21187721; <http://dx.doi.org/10.4161/auto.7.3.14348>
- [33] Koyano F, Okatsu K, Kosako H, Tamura Y, Go E, Kimura M, Kimura Y, Tsuchiya H, Yoshihara H, Hirokawa T, et al. Ubiquitin is phosphorylated by PINK1 to activate parkin. *Nature* 2014; 510:162-6; PMID:24784582
- [34] Lazarou M, Sliter DA, Kane LA, Sarraf SA, Wang C, Burman JL, Sideris DP, Fogel AI, Youle RJ. The ubiquitin kinase PINK1 recruits autophagy receptors to induce mitophagy. *Nature* 2015; 524:309-14; PMID:26266977; <http://dx.doi.org/10.1038/nature14893>
- [35] Hasuwa H, Muro Y, Ikawa M, Kato N, Tsujimoto Y, Okabe M. Transgenic mouse sperm that have green acrosome and red mitochondria allow visualization of sperm and their acrosome reaction in vivo. *Exp Anim* 2010; 59:105-7; PMID:20224175; <http://dx.doi.org/10.1538/expanim.59.105>
- [36] Mizushima N, Yamamoto A, Matsui M, Yoshimori T, Ohsumi Y. In vivo analysis of autophagy in response to nutrient starvation using transgenic mice expressing a fluorescent autophagosome marker. *Mol Biol Cell* 2004; 15:1101-11; PMID:14699058; <http://dx.doi.org/10.1091/mbc.E03-09-0704>
- [37] Takahashi K, Yamanaka S. Induction of pluripotent stem cells from mouse embryonic and adult fibroblast cultures by defined factors. *Cell* 2006; 126:663-76; PMID:16904174; <http://dx.doi.org/10.1016/j.cell.2006.07.024>
- [38] Vernia S, Cavanagh-Kyros J, Garcia-Haro L, Sabio G, Barrett T, Jung DY, Kim JK, Xu J, Shulha HP, Garber M, et al. The PPARalpha-FGF21 hormone axis contributes to metabolic regulation by the hepatic JNK signaling pathway. *Cell Metab* 2014; 20:512-25; PMID:25043817; <http://dx.doi.org/10.1016/j.cmet.2014.06.010>
- [39] Zhao T, Zhang ZN, Westenskow PD, Todorova D, Hu Z, Lin T, Rong Z, Kim J, He J, Wang M, et al. Humanized mice reveal differential immunogenicity of cells derived from autologous induced pluripotent stem cells. *Cell Stem Cell* 2015; 17:353-9; PMID:26299572; <http://dx.doi.org/10.1016/j.stem.2015.07.021>
- [40] Zhao T, Zhang ZN, Rong Z, Xu Y. Immunogenicity of induced pluripotent stem cells. *Nature* 2011; 474:212-5; PMID:21572395; <http://dx.doi.org/10.1038/nature10135>